ChE curriculum

TRIANGULAR DIAGRAMS TEACH STEADY AND DYNAMIC BEHAVIOUR OF CATALYTIC REACTIONS

K. KLUSACEK*, R. R. HUDGINS,
and P. L. SILVESTON
University of Waterloo
Waterloo, Ontario, Canada, N2L 3G1

BY THE TIME students take their first reaction engineering course, they have usually become very familiar with triangular diagrams. These are often introduced in the first or second year stoichiometry courses and are a part of physical chemistry and most engineering thermodynamics courses.

Triangular diagrams turn out to be quite useful in illustrating the dynamic behaviour of heterogeneous catalytic reactors. Thus, there is a good case for introducing them into an undergraduate chemical reaction engineering course.

The purpose of this article is to illustrate how the triangular diagram can aid in presenting some of the rather complex transient interactions that occur among gas and surface species during heterogeneous catalytic reactions. To avoid undue complexity, we assume a catalyst bed in which there are no limitations of transport either in or around the catalyst particles. Both CSTR's and differential reactors are described by identical equations for a gradientless system in the following derivation so what follows applies to both reactor types.

In chemical reaction engineering, triangular diagrams are used to represent selectivity in complex reactions. Wei and Prater [1] seem to have pioneered their use to illustrate the course of a complex homogeneous reaction sequence. States of the system rather than time appear in triangular diagrams. Occasionally, these diagrams have appeared in textbooks [2, 3], but usually in conjunction with an example. We have not seen their use for heterogeneous catalytic reactions, the subject of this article.

The triangular diagram is helpful for showing the progress of the reaction both in the gas phase and on the catalyst surface. It provides a wealth of information that is hard to present otherwise.

BASIC EQUATIONS

Figure 1 is a schematic diagram of a reactor with an ideally mixed gas phase. Let us suppose that in the reactor k gaseous components A_i (i = 1,...,k) are present with molar concentrations c_i^0 (mol/mL) at the reactor inlet and c_i at the reactor outlet (equal to the concentrations inside the reactor). Components A_j (j = k+1,...,n) are adsorbed on the catalyst surface with molar concentrations c_j (mol/g_{cat}).

The reactor has a gas phase volume V (mL) and

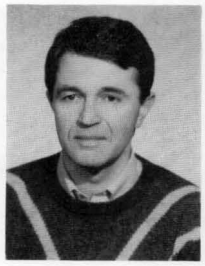

Karel Klusacek is a senior scientist at the Institute of Chemical Process Fundamentals in Prague, Czechoslovakia. He has degrees from the Technical University in Prague and from the Czechoslovak Academy of Sciences. His research focuses on the dynamics of catalytic reactors and bioreactors, and regeneration of industrial catalysts.

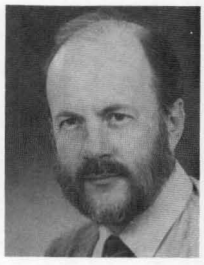

Bob Hudgins is a professor of chemical engineering at the University of Waterloo, Canada, and holds degrees from the University of Toronto and Princeton University. He teaches reaction engineering, staged operations, and laboratories that go with them. His research interests lie in periodic operation of catalytic reactors and in the improvement of gravity clarifiers.

P. L. Silveston has been at the University of Waterloo since 1963. Originally from the U.S. he was educated at M.I.T. and the Technical University of Munich (West Germany). His teaching activities have been in reactor engineering, thermodynamics, engineering economics, process design, and entrepreneurship. Research interests are in the cyclic forcing of chemical reactor and coal carbonization and gasification.

*Institute of Chemical Process Fundamentals. Czechoslovak Academy of Sciences, 165 02 Prague 6, Czechoslovakia

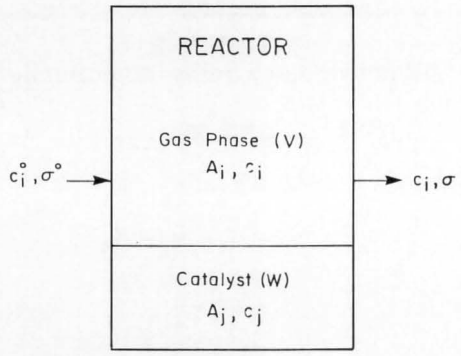

FIGURE 1. Reactor scheme

contains a stationary catalyst bed of weight W (g), the whole reactor system being maintained at constant temperature and pressure. The reaction mixture is introduced into the reactor with the inlet space velocity σ^0 (s^{-1}), defined as the ratio of the volumetric flow rate and reactor volume, and leaves the reactor with the outlet space velocity σ. Generally $\sigma \neq \sigma^0$ because the total number of moles may be changed by the reaction and, in unsteady operation, because of adsorption and/or desorption processes. Mass balances on the reaction components in the fluid phase of the reactor give k differential equations

$$\left(\frac{dc_i}{dt}\right) = \sigma^o c_i^0 - \sigma c_i + \left(\frac{W}{V}\right) R_i; \qquad i = 1,\ldots,k \qquad (1)$$

where R_i ($mol/g_{cat} \cdot s$) is the rate of formation of any gaseous component A_i ($i = 1,\ldots,k$) and t(s) is time. Similarly, for the components on the catalyst surface, we have

$$\left(\frac{dc_j}{dt}\right) = R_j; \qquad j = k+1,\ldots,n \qquad (2)$$

Concentrations in the reactor fluid phase sum to the total molar concentration, c_T (mol/mL), while those on the surface and any free sites sum to the total concentration of the active sites (assumed constant here) on the catalyst surface, c_L(mol/g_{cat}). The set of n balance Eqs. (1) and (2) is complemented by the initial conditions, for the n species. The mass balance equations may be recast in dimensionless form as follows

$$\left(\frac{da_i}{d\tau}\right) = a_i - \left(\frac{\sigma}{\sigma^0}\right) a_i + \phi\rho_i; \qquad i = 1,\ldots,k \qquad (3)$$

and

$$\left(\frac{da_j}{d\tau}\right) = \rho_j; \qquad j = k+1,\ldots,n \qquad (4)$$

Dimensionless variables used in Eqs. (3) and (4) are

Triangular diagrams turn out to be quite useful in illustrating the dynamic behaviour of heterogeneous catalytic reactors. Thus, there is a good case for introducing them into an undergraduate chemical reaction engineering course.

TABLE 1
Dimensionless Variables

Variable	Definition
dimensionless bulk concentration at the reactor inlet	$a_i^o = c_i^o/c_T$; $i = 1,\ldots,k$
dimensionless bulk concentration in the reactor	$a_i = c_i/c_T$; $i = 1,\ldots,k$
dimensionless concentration on the catalyst surface	$a_j = c_j/c_L$; $j = k+1,\ldots n$
dimensionless time	$\tau = t\sigma^0$
dimensionless rate of formation of gaseous component A_i	$\rho_i = R_i/(c_L\sigma^0)$; $i = 1,\ldots k$
dimensionless rate of formation of surface component A_j	$\rho_j = R_j/(c_L\sigma^0)$; $j = k+1,\ldots,n$
capacity factor	$\phi = W_{cL}/(V_{cT})$ (molar capacity of catalyst surface/molar capacity of fluid phase)

summarized in Table 1. The material balances, Eq. (3), contain the space velocity at the reactor outlet, σ, which can be determined only with difficulty. This quantity can be expressed as the function of the space velocity at the reactor inlet, σ^0, by summing the k equations [Eq. (3)] and noting that the summation of derivatives must equal to zero. After rearrangement

$$\sigma = \sigma^0\left[1 + \phi\sum_{i=1}^{k} \rho_i\right] \qquad (5)$$

The solution of the model for initial conditions gives the time profiles of concentrations in the reactor gas phase as well as on the catalyst surface either for steady state or during transient operation of the reactor. What triangular diagrams show may be seen from the following example.

NUMERICAL EXAMPLE

Kinetic model

Consider a simple irreversible heterogeneous catalytic reaction between gaseous components A and

B forming gaseous product C proceeding via the following elementary steps

(adsorption/desorption of A)

$$A + S \underset{k_1'}{\overset{k_1}{\rightleftharpoons}} A \cdot S \qquad (6a)$$

(adsorption/desorption of B)

$$B + S \underset{k_2'}{\overset{k_2}{\rightleftharpoons}} B \cdot S \qquad (6b)$$

(surface reaction)

$$A \cdot S + B \cdot S \xrightarrow{k_3} C + 2S \qquad (6c)$$

Forward and reverse reaction rate constants are denoted as k_i and k_i', respectively. Gaseous components are represented as

$$A \equiv A_1; \quad B \equiv A_2; \quad C \equiv A_3$$

and for components on the catalyst surface

$$A \cdot S \equiv A_4; \quad B \cdot S \equiv A_5; \quad S \equiv A_6$$

The dimensionless rates of formation of individual components are given in Table 2, while the dimensionless rate constants with numerical values are shown in Table 3.

Defining the normalized rate of product formation, ρ, as the ratio of actual to maximum possible rates, ρ_3, where the maximum possible rate of product formation, $\rho_{3,max}$, is attained for $a_4 = a_5 = 0.5$,

$$\rho = \frac{a_4 a_5}{(a_4 a_5)_{max}} = \frac{a_4 a_5}{(0.5)(0.5)} = 4 a_4 a_5 \qquad (7)$$

The material balance [Eqs. (3) and (4)] for $k = 3$ and $n = 6$ can then be used to simulate steady-state and transient behaviour of the A + B → C catalytic reaction in a CSTR. The values of the parameters used for numerical calculations are as follows: W = 5 g, V = 10 mL, $c_T = 2.437 \times 10^{-5}$ mol/mL, $c_L = 1.0 \times 10^{-4}$ mol/g. The dimensionless rate constants K_i (i = 1, 2, 3) and K_j' (j = 1,2) are dependent on the space velocity σ^0 (see Table 3). Thus, numerical values of rate constants in Table 3 correspond to the space velocity, $\sigma^0 = 1.0\ s^{-1}$. The value of the total molar concentration, c_T, follows from its definition, $c_T = P/(RT)$, for P = 101.3 kPa and T = 500 K.

Steady-state reactor behaviour

At steady-state, the derivatives (accumulation terms) on the left side of Eqs. (3) and (4) are equal to zero, reducing the set of coupled differential equations

TABLE 2
Dimensionless rates of Formation

Rate	Definition
ρ_1	$-K_1 a_1 a_6 + K_1' a_4$
ρ_2	$-K_2 a_2 a_6 + K_2' a_5$
ρ_3	$K_3 a_4 a_5$
ρ_4	$-(\rho_1 + \rho_3)$
ρ_5	$-(\rho_2 + \rho_3)$
ρ_6	$-(\rho_4 + \rho_5)$

TABLE 3
Dimensionless Rate Constants

Constant	Definition	Numerical Value
K_1	$(c_T/\sigma^0)k_1$	1.00
K_1'	$(1/\sigma^0)k_1'$	0.05
K_2	$(c_T/\sigma^0)k_2$	0.30
K_2'	$(1/\sigma^0)k_2'$	0.10
K_3	$(c_L/\sigma^0)k_3$	0.10

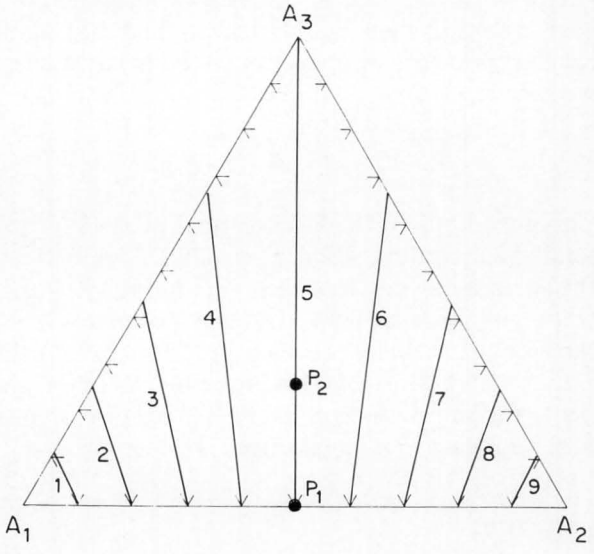

FIGURE 2. Steady-state gas concentrations in the reactor for different feed compositions, a_1^0 / a_2^0

(1) 0.9/0.1 (2) 0.8/0.2 (3) 0.7/0.3
(4) 0.6/0.4 (5) 0.5/0.5 (6) 0.4/0.6
(7) 0.3/0.7 (8) 0.2/0.8 (9) 0.1/0.9

to algebraic ones. Because of the nonlinearity resulting from the reaction rate expressions the system has to be solved numerically (see for example, Ralston [4]).

Figure 2 shows typical results for the bulk phase of the reactor for different feed composition ratios a_1^0/a_2^0. For example, let us suppose that the reaction mixture at the reactor inlet has the stoichiometric composition $a_1^0 = a_2^0 = 0.5$ (no product A_3 is present). This composition corresponds to the point P_1 on the diagram. Depending on the space velocity, σ^0, used, the composition of the gaseous phase in the reactor will move along the line P_1A_3. For example, for $\sigma^0 = 0.03$ s^{-1}, the steady-state composition of the reactor gas phase is given by the point P_2 ($a_1 = 0.22$, $a_2 = 0.22$, $a_3 = 0.56$).

The smaller σ^0 is the closer to the point A_3 the resulting composition will be. For infinitesimal σ^0, full conversion of reaction components will be attained and only pure product A_3 will be present in the reactor. For non-stoichiometric inlet compositions, the resulting reaction mixture will always contain unreacted components A_1 and/or A_2 as is shown in Figure 2. The location of the composition point will again depend on the space velocity used.

Figure 3 gives the catalyst surface concentrations corresponding to the gas-phase concentrations in Figure 2. The asymmetry of Figure 3 is striking and is a direct result of the fact that A_1 is more strongly adsorbed on the catalyst than A_2 (*cf.* values of rate constants in Table 3).

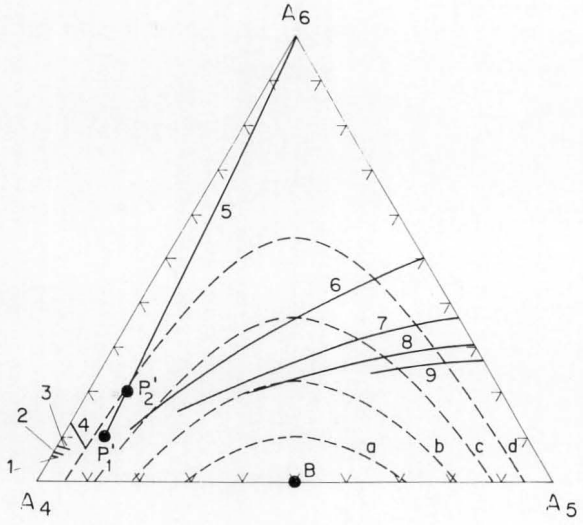

FIGURE 3. Steady-state surface concentration for different feed compositions, a_1^0 / a_2^0

(1) 0.9/0.1	(2) 0.8/0.2	(3) 0.7/0.3
(4) 0.6/0.4	(5) 0.5/0.5	(6) 0.4/0.6
(7) 0.3/0.7	(8) 0.2/0.8	(9) 0.1/0.9

Lines of constant normalised rate, ρ (dashed lines):

(a) ρ = 0.8 (b) ρ = 0.6 (c) ρ = 0.4 (d) ρ = 0.2

As in Figure 2 the steady-state combination of the surface concentrations depends on the space velocity. The origins of the surface concentration lines have been calculated for a very high space velocity ($\sigma^0 = 1 \times 10^6$ s^{-1}) for which the composition of the reaction mixture leaving the reactor is essentially the feed composition (zero conversion). The feed composition ratios lying along axis A_1A_2 in Figure 2 do not correspond to the axis A_4A_5 in Figure 3. Instead, they correspond to surface concentrations along a curve formed by joining the lowest points in lines 1 to 9. This curve then accounts for the number of unoccupied catalyst sites (A_6) which varies with the feed composition. For example, the surface concentrations for the fluid-phase composition, given by the point P_1 ($a_1^0 = a_2^0 = a_1 = a_2 = 0.5$) in Figure 2, is denoted as P_1' in Figure 3 ($a_4 = 0.82$, $a_5 = 0.08$). The gas phase concentration given by the point P_2 in Figure 2 corresponds to point P_2' in Figure 3. For stoichiometric feed, the composition on the catalyst surface will follow line 5 in Figure 3, finally attaining the vertex A_6. This point corresponds to the total conversion of both reaction components A_1 and A_2 (product A_3 is not adsorbed).

The normalized steady-state rate ρ (Eq. 7) is proportional to the product of surface concentrations a_4 and a_5. The dashed curves in Figure 3 are lines of normalized rate $\rho = 4a_4a_5$. The highest value of ρ occurs at point B ($a_4 = a_5 = 0.5$; $\rho = 1$); and ρ decreases with increasing distance from B (*i.e.*, with increasing space velocity). The curves depicted in Figure 4 for two different feed compositions are typical of the steady-state rate surface.

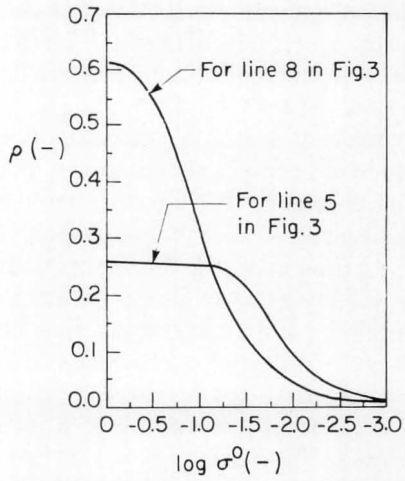

FIGURE 4. Steady-state normalized rates, ρ, for different space velocities, σ^0 and two feed compositions, a_1^0 / a_2^0, corresponding to line 5 in Figure 3 and line 8 in Figure 3.

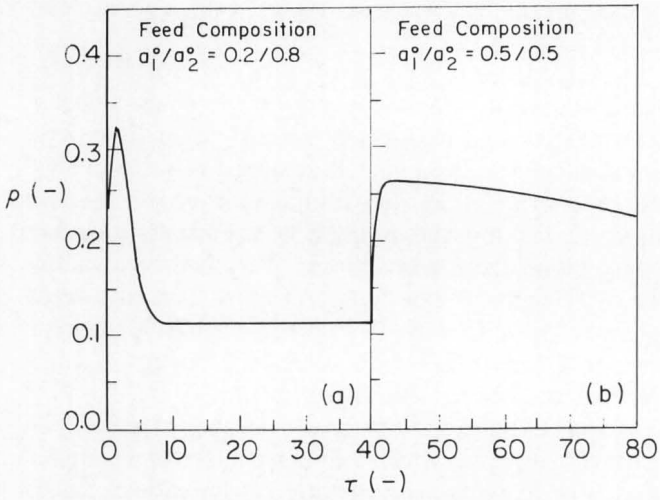

FIGURE 5. Transient of normalized rate, ρ, after step-change of feed composition a_1^0 / a_2^0

(a) a_1^0/a_2^0 = 0.5/0.5 —step-change→ a_1^0/a_2^0 = 0.2/0.8
(b) a_1^0/a_2^0 = 0.2/0.8 —step-change→ a_1^0/a_2^0 = 0.5/0.5

Transient Reactor Behaviour

In general, a catalytic reactor seldom operates under ideal steady-state conditions. Small random fluctuations of the system variables (*e.g.*, temperature, pressure, space velocity, and composition) and changes in the catalyst activity are common. Another kind of transient reactor behaviour occurs after the forced change of either feed composition or reactor temperature. Analysis of forced transient reactor behaviour can furnish mechanistic information (such as the surface populations during reaction) that cannot be obtained from steady-state data.

In the following example, a step-change of the feed composition is used. The dynamic operation of the reactor can be predicted by the numerical integration of balance Eqs. (3) and (4).

The normalized transient rate, ρ, after a step-change in the feed composition is shown in Figures 5a and 5b. The reactor is initially at steady-state with feed composition $a_1^0 = a_2^0 = 0.5$, and space velocity $\sigma^0 = 0.03\ s^{-1}$. At time zero, the feed composition is stepped to $a_1^0 = 0.2$, $a_2^0 = 0.8$ while σ^0 remains unchanged. After the period $\tau = 40$, the original feed composition ($a_1^0 = a_2^0 = 0.5$) is restored. The effect of switching the feed composition can be seen in Figure 5a. An overshoot in ρ occurs immediately after the step-change of input. The maximum is reached at $\tau = 2$. Figure 6 illustrates the changes occurring on the catalyst surface for the cycle given in Figure 5, and explains the overshoot. The value of ρ is proportional to $a_4 \times a_5$. The starting point P_1', being low in component A_5 on the catalyst surface, is not conducive to a high rate of product A_3 formation. Immediately after the feed step-change, the value of a_4 suddenly decreases as a result of the low concentration of A_1 in the feed ($a_1^0 = 0.2$). Thus the surface concentration of A_5 increases and moves towards the region of higher ρ. The direction of the movement of the surface concentration is illustrated by the arrows in Figure 6. These surface changes lead immediately to a reduced surface coverage (A_6 = free centers) and a higher value of the rate ($\rho = a_4 a_5$). For dimensionless time $\tau > 2$, the surface concentration a_4 becomes small and the rate ρ decreases. At $\tau = 40$, the catalyst reactor reaches a new steady-state (point P_3') and at this time the feed composition is stepped back to the original value ($a_1^0 = a_2^0 = 0.5$). The processes on the catalyst surface are represented by the closed trajectory returning from point P_3' to P_1'. At time $\tau = 80$, the system resumes its original steady-state (point P_1').

Figure 6 thus illustrates that the surface, passing between two separate steady states, does not follow the same path. Instead, the path depends on the direction of the change in feed composition.

CLASSROOM USE

Figures 2 and 3 illustrate the importance of the adsorption equilibrium coefficient. For the parameters used it can be seen that the compositions of the adsorbate phase and the fluid phase are very different. In a similar fashion, as the composition of the feed varies from A_1 to A_2 in Figure 2, the surface composition does not move along the axis A_4A_5 in

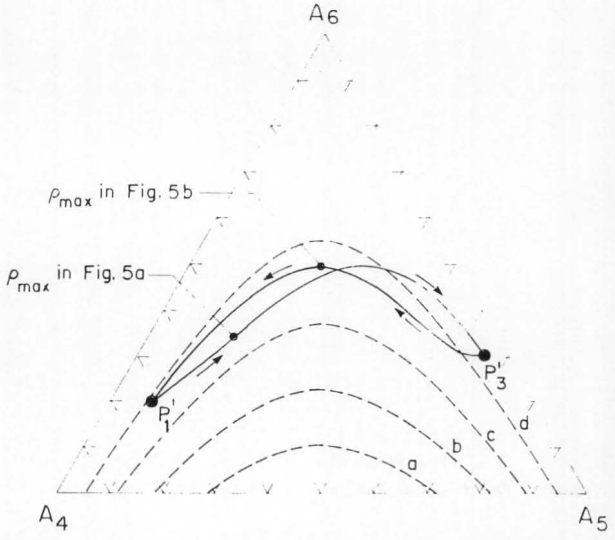

FIGURE 6. Transient of surface concentrations after step-change of feed composition as in Figure 5. Lines of constant normalized rate, ρ (dashed lines);

(a) ρ = 0.8 (b) ρ = 0.6 (c) ρ = 0.4 (d) ρ = 0.2

Figure 3; instead, it follows a curved path given by the locus of the lowest points of the numbered lines in Figure 3 as discussed above.

Normally students conceive of reactions in terms of the microreversibility theorem and would assume that the reverse path following a reversal of the step-change would be the same as the forward path. Figures 5 and 6 show that this is not the case. Thus. microreversibility is inappropriate for describing surface concentrations in this and similar systems.

An exercise that students will find interesting is to calculate the surface composition for a non-reaction system and a reacting one even if the rate constants are very small. Will these compositions be identical?

CONCLUSIONS

Triangular diagrams are useful for teaching steady-state and transient reactor behaviour of catalytic reaction models. Concentrations of surface species, not normally measurable, are particularly easy to reveal and to use to suggest interpretations of transient operation. Similar calculations can, of course, be performed for catalytic reactions with arbitrary mechanisms. In the example presented, the transient reactor behaviour was excited by the step-change of feed composition. Other types of steady-state feed disturbances (*e.g.*, sine, ramp, *etc.*) can be used after proper formulation of the initial conditions.

For systems having more than three components. appropriate subsystems of variables may be chosen. The main advantage of the triangular diagram lies in its power to compress into understandable form a great deal of information about the progress of gas and surface species in catalytic reaction. The FORTRAN programs used in this study are available from the authors.

ACKNOWLEDGEMENTS

The authors are grateful for support through the Natural Sciences and Engineering Research Council of Canada in the form of an International Scientific Exchange Award (to K.K.) and an operating grant (to R.R.H.).

REFERENCES

1. Wei, J., and C. D. Prater, "The Structure and Analysis of Complex Reaction Systems," *Advances in Catalysis,* **13**, Academic Press, New York (1965)
2. Westerterp, K. R., W.P.M. van Swaaij, and A.A.C.M. Beenackers, *Chemical Reactor Design and Operation,* John Wiley & Sons, New York (1983)
3. Fogler, H.S., *Elements of Chemical Reaction Engineering,* Prentice-Hall, Englewood Cliffs, NJ (1986)
4. Ralston, A., *A First Course in Numerical Analysis,* McGraw-Hill, New York (1965) ❐

REVIEW: Transport Phenomena

Continued from page 175.

I would like to single out a few papers that are worth extended attention. The keynote lectures all fall into this class, although their coverage varies considerably. They do provide the reader a wealth of information gathered by the authors. In addition, on coherent structures, Blackwelder's short post-conference note is noteworthy. Criminale's contribution offers new insight. Other noteworthy contributions are by Walker and Herzog, and Nishino, *et al.* On wall shear flows, the contributions by Nagano and Tagawa, Usui and Sano, and Ueda *et al.*, should receive more than casual consideration. On free shear flows, I enjoyed reading contributions by Tabatabai *et al.*, Stapountzis, and Kobayashi *et al.* Since I have a special interest in scalar transport, I read all of these. My knowledge of modeling details is more limited; these papers appear to be of interest to one involved in transport modeling, a necessity in our modern engineering society. The numerical simulations of turbulence and transport is a new and budding field; thus contributions rapidly become dated. The two keynote lectures form a good starting place, and the general contributions add to them. Measuring techniques are varied and should receive the researcher's careful attention. The ideas advanced by Bawirzanski *et al.*, Ciccone *et al.*, Akino *et al.*, and Hardalupas *et al.*, are all worthwhile contributions. ❐

BUOYANCY-INDUCED FLOWS AND TRANSPORT

by Benjamin Gebhart, Yogesh Jaluria, Roop L. Mahajan, and Bahgat Sammakia
Hemisphere Publishing Corp., 79 Madison Ave., New York, NY 10016; 1001 pages, $95 (cloth); 971 pages, $49 (paperback); 1988

Reviewed by
J. S. Vrentas
The Pennsylvania State University

With seventeen chapters and more than nine hundred pages, this book deals with a wide range of buoyancy-induced flow problems. The analysis of steady and unsteady laminar external flows driven by both thermal and concentration effects is the focus of the first third of the book. Fluid property variations, turbulence, mixed convection, non-Newtonian effects, and the characteristics of instabilities are considered in subsequent chapters. Buoyancy-driven motions in fluid layers and in enclosures as well as natural convection in porous media are also discussed. Since problems are presented at the end of each chapter, this book can be used not only as a reference source but also as a textbook for a graduate specialty course. A significant part of the book could be covered in a one-semester course at the graduate level.

The authors present their analysis from an engi-

Continued on page 193.